Liquid crystal 8CB in random porous glass: NMR relaxometry study of molecular diffusion and director fluctuations

M. Vilfan,[1,*] T. Apih,[1] P. J. Sebastião,[2,3,†] G. Lahajnar,[1] and S. Žumer[1,4]

[1]*Jozef Stefan Institute, Jamova 39, SI-1000 Ljubljana, Slovenia*
[2]*Centro de Física da Matéria Condensada, Avenida Prof. Gama Pinto 2, 1649-003 Lisbon, Portugal*
[3]*Department of Physics, IST, TU Lisbon, Av. Rovisco Pais, 1049-001 Lisbon, Portugal*
[4]*Department of Physics, University of Ljubljana, Jadranska 19, SI-1000 Ljubljana, Slovenia*
(Received 17 July 2007; published 30 November 2007)

We present the measurements of the proton spin-lattice relaxation time T_1 of liquid crystal 4-*n*-octyl-4′-cyanobiphenyl (8CB) confined into randomly oriented ~15 nm pores of untreated porous glass. In the low kilohertz range the spin-lattice relaxation rate in the nanoconfined 8CB is about ten times larger than in the bulk. We show that the increase is mainly due to molecular reorientations mediated by translational displacements (RMTD). In the paranematic phase the power law describing the RMTD dispersion, $(T_1^{-1})_{RMTD} \propto \omega^{-p}$, is well characterized by the exponent $p = 0.5 \pm 0.06$ and suggests an equipartition of diffusion modes with different wavelengths. The largest distance related to the decay of the orientational correlation function is about twice the diameter of the cavity. The situation is different in the nematic phase, where the orientational correlation is eventually lost at ~60 nm in the direction along the pore, a distance corresponding roughly to the length of a pore segment in the glassy matrix. The exponent p is between 0.65 and 0.9, depending on the temperature, which implies that in the nematic phase long wavelength modes are relatively more important—a consequence of the uniform director field along the pore. These observations are in agreement with the model of mutually independent pores with nematic director parallel to the pore axis in each segment. We point out that in strongly confined liquid crystals the proton NMR relaxometry does not provide the evidence of director fluctuations correlated over micrometer distances as was suggested earlier. The local translational diffusion of molecules within the cavities is found about as fast as in bulk.

I. INTRODUCTION

Nuclear magnetic resonance (NMR) spectroscopy and relaxometry are by now well established experimental techniques to study orientational order and dynamics of liquid crystals in random porous media. NMR spectra of deuterons [1–5], protons [6], carbon 13 [6], and xenon [7] nuclei have been measured and analyzed in order to establish the impact of liquid crystal surface interactions and topological constraints on the ordering and phase transitions in such systems. It is well known that the NMR spectra clearly demonstrate the existence of weak orientational order at temperatures above the bulk clearing point T_{NI} and reveal a substantial suppression of the nematic-isotropic transition in cavities smaller than ~15 nm. In such cavities there is a continuous evolution of orientational order with decreasing temperature. Its maximum rate of growth takes place several K below T_{NI}, depending on the size of the enclosures. On the other hand, conclusions on the magnitude of local orientational order and on the correlation lengths of director and orientational order parameter cannot be straightforwardly drawn from the macroscopic NMR observables. It is particularly difficult to discriminate correctly the influences of ordering and translational diffusion when interpreting the line shapes at temperatures close to the bulk clearing point. Nuclear spin relaxometry can be a helpful complementary

method to obtain information on molecular dynamics and to clear up the onset and nature of orientational order [8–10]. It usually includes the measurements of the spin-lattice relaxation time T_1, recorded over a broad frequency range, and the transverse spin relaxation time T_2.

In this paper we focus on the *proton spin-lattice relaxation* of a liquid crystal confined into random porous glass. The spin-lattice relaxation rate T_1^{-1} reflects—when measured at different Larmor frequencies—a broad spectrum of molecular dynamics. At megahertz Larmor frequencies, T_1^{-1} is mainly determined by individual molecular reorientations and by the local molecular translational displacements [11]. Both dynamic processes are usually classified as "fast molecular motions" in the NMR terminology of liquid crystals. To get an insight into the kilohertz frequency regime and "slow" molecular dynamics, a special technique, fast field-cycling NMR, is applied [12–14]. It allows the measurements of T_1 in the frequency range of four decades between ~1 kHz and ~10 MHz without losing the strength of the signal which is detected in the high magnetic field.

The first field-cycling T_1 measurements of liquid crystals in porous glasses were performed by Grinberg *et al.* [15]. They found a drastic increase in the proton spin-lattice relaxation rate in the confined sample with respect to the bulk counterpart. Terekhov *et al.* followed with the studies of nematic 5CB confined into porous glasses with different sizes of enclosures [16]. They pointed out that the increase in the relaxation rate, larger in smaller pores, is mainly due to molecular reorientations induced by translational diffusion and to a considerable slowing down of molecules next to the

*mika.vilfan@ijs.si
†pedros@lince.cii.fc.ul.pt

surface. These effects were treated in a simple form with only one correlation time involved. Using Monte Carlo simulations, Grinberg *et al.* extended the model of reorientations mediated by translational diffusion by taking into account the effects of the molecular exchange and director modulation [9,17]. It was applied to nematic 5CB in pores of only a few nanometers in diameter [17]. At variance, Leon *et al.* argue that the relaxation in the nematic phase within xero- and aerogel nanocavities results from director fluctuations and reveals the fractal nature of the inner glassy surface [18]. Their conclusion is drawn on the basis of the T_1^{-1} frequency dispersion exponent 2/3, which is different from the exponent 1/2 characteristic for the bulk nematic phase. Recently, the isotropic phase of a nematic liquid crystal in mesoscopic cavities of porous glass with diameter ~70 nm was investigated by Sebastiao *et al.* [19]. Analyzing T_1^{-1} dispersions they determined the profile of the surface induced order and clarified the type of the surface alignment which turned out to be random planar.

In the present work we are interested particularly in the ability of NMR relaxometry to elucidate the orientational ordering, fluctuations, and the role of translational diffusion in nanoconfined liquid crystals. Following this issue, we present the measurements and a comprehensive quantitative analysis of proton spin-lattice relaxation rates for 4-*n*-octyl-4′-cyanobiphenyl (8CB) confined into controlled pore glass (CPG) with average pore diameter ~15 nm. 8CB is a widely studied liquid crystal with well known macroscopic parameters and exhibits—in addition to the nematic and isotropic phases—also the smectic-*A* phase. A CPG matrix consists of randomly oriented interconnected voids of roughly cylindrical shape with a relatively uniform diameter. Its geometry is better defined than in other random porous media like aerogels, xerogels, and aerosil emulsions. The T_1^{-1} frequency dispersions of the confined 8CB were recorded at temperatures corresponding to the bulk isotropic, nematic, and smectic-*A* phases. The latter phase has been included in view of the increased interest in the nematic-smectic-*A* transition in the last years [20–23]. In the analysis of T_1^{-1} dispersions we include fast molecular motions and revisit the role of the two main slow dynamic processes, order director fluctuations (ODFs) and reorientations mediated by translational displacements (RMTDs). In the former studies there have been some inconsistencies related to the importance of translational diffusion effects, which are, however, essential in drawing conclusions on the extent of long-range orientational order.

It should be mentioned that dielectric spectroscopy studies of confined liquid crystals cover partly the same dynamic range as NMR relaxometry [6,24–26]. Our results on the local molecular reorientations can be therefore compared with those of dielectric measurements. It should be noted that NMR relaxometry detects also the RMTD dynamics which is hidden in the dielectric spectra [6].

Though the *transverse spin relaxation* of liquid crystals in random porous media is not a topic of this paper, some results have been obtained—using this complementary method—which are relevant for the discussion of spin-lattice relaxometry results. An important point related to the trans-

verse spin relaxation time T_2 is its property to contribute to the homogeneous broadening of the absorption lines in the NMR spectrum, $\Delta \nu_{hom} = (\pi T_2)^{-1}$ [12]. As a rule, above and below the bulk clearing point, the deuteron NMR spectrum of a liquid crystal in random nanometer pores consists of a single line which is broadened with respect to the bulk. Apart from the effect of local magnetic field inhomogeneities, the broadening might be either homogeneous, related to the transverse spin relaxation time, or resulting from the residual static quadrupole interactions. In the case of homogeneous broadening, which is provoked by the diffusion of molecules traveling along randomly oriented enclosures, the linewidth is proportional to the square of the order parameter S, whereas it is linear in S in the case of static broadening. Combining NMR line shape and transverse spin relaxation rate it was found that the observed continous linewidth broadening in CPG is mainly due to diffusion averaging effects and to a lesser extent due to the glasslike freeze-out of orientational order [10,27]. Local molecular translational diffusion should be almost as fast as in the bulk, except, probably, in the first molecular layer next to the wall. Such a nonhindered local diffusion is not in contradiction with the results of direct measurements of the diffusion coefficient using pulsed-field-gradient NMR method [10]. A ten times smaller diffusion coefficient obtained by that method measures, namely, the diffusion over a much larger time interval than NMR relaxometry and reflects therefore the effect of the tortuosity of the sample and not a possible local slowing down of translational diffusion.

The present paper is organized as follows. In Sec. II we describe the experiment and present the measurements of the temperature and frequency dependences of the proton spin-lattice relaxation rates T_1^{-1} for 8CB in ~15 nm CPG and in the bulk. In the next section, we discuss relaxation mechanisms for randomly confined liquid crystals and present the models relevant for their description. We calculate, in particular, the spin-lattice relaxation rate induced by director fluctuations in a space of arbitrary dimension and compare the result with the known limiting cases for dimensionalities of integer number. In Sec. IV, T_1^{-1} dispersions at several temperatures, corresponding to the bulk isotropic, nematic, and smectic-*A* phases, are quantitatively analyzed in terms of relaxation models specific for the randomly confined liquid crystals. We show that rotations mediated by translational displacements are the leading relaxation mechanism in the low kHz range. The fitted parameters throw some light on the director correlation length, translational self-diffusion, and surface anchoring. A summary is given in Sec. V.

II. EXPERIMENT

Liquid crystal used in the present study is the common 8CB (4-*n*-octyl-4′-cyanobiphenyl), purchased from Sigma-Aldrich Chemie GmbH, and used without further purification. Controlled pore glass (CPG Inc., New Jersey) was used as the porous matrix. It consists of porous grains of the size ~200–800 μm. From a scanning electron micrograph [Fig. 1(a)], CPG grains can be described as networks of three-dimensional randomly oriented and interconnected pore seg-
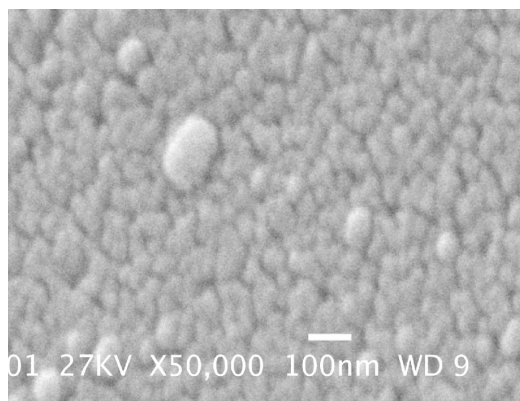
(a)
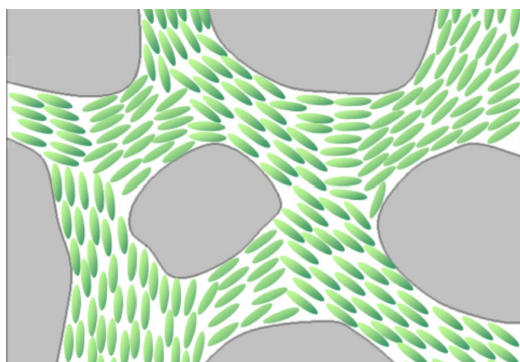
(b)

FIG. 1. (Color online) Scanning electron micrograph (SEM) of the empty controlled pore glass (CPG) with average pore diameter ∼15 nm (a), and a schematic presentation of liquid crystal molecules confined into porous glass (b). An inspection of the SEM micrograph shows that the lengths of pore segments are roughly between ∼50 and ∼100 nm. The micrograph was provided by the Department of Nanostructured Materials at the J. Stefan Institute. The schematic picture given in Fig. 1(b) represents the model with director oriented everywhere along the pores and with the homogeneous orientational order parameter in the system.

ments. According to the specifications of CPG Inc. the pores have a relatively uniform diameter, ∼15 nm. The length of the pore segments—estimated from the inspection of Fig. 1(a)—is between 50 and 100 nm. The NMR sample was prepared by immersing the CPG grains into a mixture of concentrated sulphuric and nitric acids, followed by an extensive washing with distilled deionized water, setting under a modest vacuum, and drying at 250 °C for 24 h. In the filling procedure, an amount of 8CB, corresponding to the volume of the pores, was soaked into the CPG grains at a temperature where 8CB is in the isotropic phase. The material was then transferred into the NMR tube with diameter 8 mm, set under vacuum, and sealed.

As seen by atomic force microscopy, the inner surfaces of the CPG cavities are smooth to the nanometer scale [28]. They impose tangential orientation of liquid crystal molecules to the surface. At temperatures above T_{NI} the nanoconfined 8CB is in the paranematic phase. The surface layer

in untreated CPG exhibits a random planar order [19]. With decreasing temperature the thickness of the ordered layer increases to extend eventually over the whole cavity. The average orientation of molecules within a pore segment in the nematic phase is relatively uniform with director parallel to the axis of the cylindrically shaped void. From the macroscopic point of view, however, the CPG matrix imposes a disorder on the liquid crystal as the orientation of local segments is random in space. The schematic presentation of a liquid crystal in CPG is given in Fig. 1(b). The magnetic coherence length of 8CB in the magnetic field 0.25 T of the NMR spectrometer is ∼18 μm; it is much larger than the diameter of the voids. The effect of magnetic field on the director orientation is therefore completely negligible.

Proton spin-lattice relaxation times T_1 at different angular Larmor frequencies ω were measured with the commercial fast field-cycling NMR relaxometer (SpinMaster FFC 2000, Stelar s.l.r., Mede, Italy). The sample was initially polarized in the high magnetic field $B_H = 0.4$ T for a time $t_{POL} > 5T_1$. Then the sequence $B_{H \to L} - \tau_i - B_{L \to H} - \pi/2$—free induction decay was applied, where τ_i is the evolution time, B_H and B_L are the high and low magnetic fields, respectively, and $\pi/2$ is the radio-frequency pulse [19]. After recording the signal, the magnetic field was switched off to provide the cooling of the magnet. Repeating the experiment for different relaxation times τ_i allows for extraction of the spin lattice-relaxation time $T_1(B_L)$, i.e., $T_1(\omega = \gamma B_L)$. The external local magnetic fields, including Earth's field, were compensated with a set of perpendicular coils. The time dependence of the magnetization curves was a monoexponential function to a good approximation indicating a uniform spin-lattice relaxation time throughout the sample. Relative error of all T_1 measurements was below 5%. The temperature of the sample was stabilized with an air flux system controlled by the Stelar VTC unit. The absolute temperature error was about 0.4 K, while the reproducibility of the measurements was below 0.2 K.

Figure 2 shows the temperature dependences of the proton T_1^{-1} of the bulk and nanoconfined 8CB on cooling. It is obvious that the specific features of different phases have a well expressed impact on the spin relaxation when measured at low Larmor frequencies. According to the spin-lattice relaxation data at 10 kHz, the isotropic-nematic transition in the bulk 8CB, which is discontinuous, takes place at 40.2 °C±0.2 °C. The nematic-smectic-A transition, which is known to be second order, is accompanied by a strong decrease in the relaxation rate at 34.3 °C±0.5 °C in agreement with the data in the literature. In the nanoconfined 8CB, the transition between the paranematic and nematic phases is observed via a significant increase in T_1^{-1}. Notably, this transition is (a) shifted toward a lower temperature with respect to the bulk and occurs at 38 °C±1 °C, and (b) it is apparently gradual. The enclosures with diameter 15 nm are close to the critical size where the first order phase transition turns into continuous growth of orientational order [2]. Still, calorimetric measurements, which have a better temperature resolution, show that 8CB in 15 nm pores experiences an extremely weak, but still discontinuous paranematic-nematic phase transition [29]. In contrast, the nematic-smectic-A transition is gradual with a slow evolution of positional order
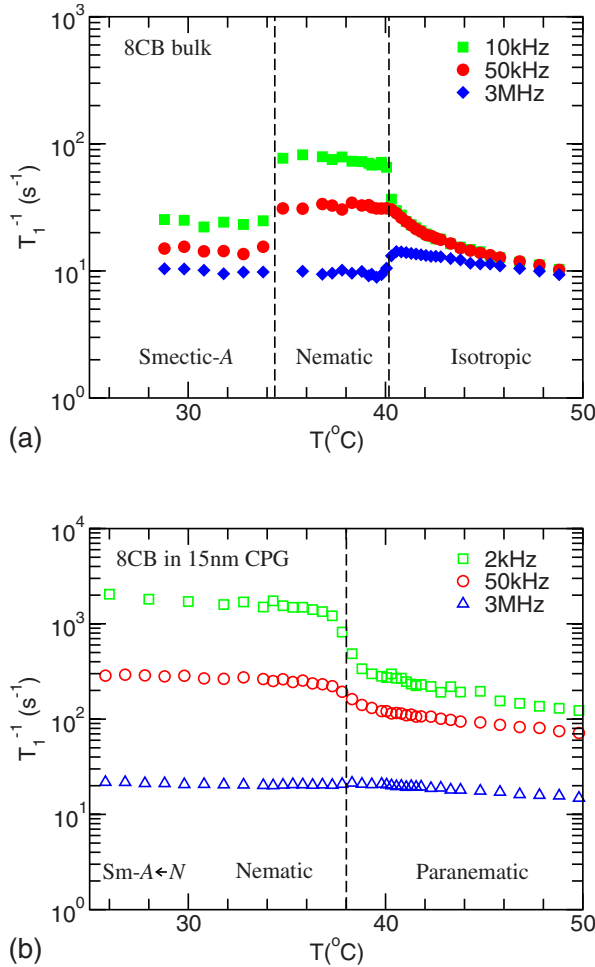
FIG. 2. (Color online) Temperature dependence of the proton spin-lattice relaxation rate T_1^{-1} at three Larmor frequencies for 8CB in the bulk (a), and in 15 nm porous glass (b) on cooling.

FIG. 3. (Color online) Frequency dependences of the proton spin-lattice relaxation rate T_1^{-1} for 8CB in the bulk (a), and in 15 nm porous glass (b) in the isotropic phase (50 °C), nematic phase (37 °C), and in the bulk smectic-A phase (28 °C). In the confined 8CB, the frequency dependence of T_1^{-1} at 28 °C falls into the temperature range where a gradual transition from the nematic into the smectic-A phase is taking place.

starting at ~29 °C [29]. No discontinuity in T_1^{-1} is observed at this temperature.

The dependences of T_1^{-1} on the Larmor frequency ν_L, i.e., dispersions, were measured in the range between 2 kHz and 10 MHz. The measurements were performed at temperatures corresponding to the isotropic, nematic, and smectic-A phases of the bulk compound (Fig. 3). In Fig. 3(a) it is clearly seen that the shape of the bulk T_1^{-1} dispersions is characteristic of each particular phase. In the isotropic phase, T_1^{-1} is virtually frequency independent in the frequency range under study. The onset of the nematic phase is marked by a strong contribution of director fluctuations with the characteristic $T_1^{-1} \propto \omega^{-1/2}$ frequency dependence. In the smectic-A phase the contribution of director fluctuations vanishes above ~10 kHz. Below this frequency a steeper increase in T_1^{-1} takes place which is usually ascribed to two-dimensional director fluctuations with $T_1^{-1} \propto \omega^{-1}$. If the smectic-A phase is not uniformly oriented along the magnetic field (as in the case of our measurements), this increase may result partly from diffusion of molecules among regions with different director orientation. The basic features of T_1^{-1} dispersions for the confined 8CB are presented in Fig. 3(b). The relaxation

rate is definitely much faster and dispersion curves have different shape from those of the bulk what indicates significant changes in the relaxation mechanisms involved.

III. RELAXATION MECHANISMS

Spin-lattice relaxation of protons occurs via the time modulation of magnetic dipole-dipole interactions of spin pairs. This process is induced by the motion of spin-bearing molecules accompanied by the reorientations of the interproton vector with respect to the magnetic field or by varying the distance between spins on neighboring molecules. In the analysis of T_1^{-1} dispersions we will take into account the following molecular motions which are acting as relaxation mechanisms:

(i) *Local molecular reorientations (R)* include rotation around the long molecular axis with the correlation time τ_L and reorientations around the short molecular axis with the

correlation time τ_S. In the isotropic phase, the contribution of these motions to the total relaxation rate, $(T_1^{-1})_R$, is given by the well known Woessner's expression for the relaxation induced by the reorientations of rigid elongated molecules [30]. Apart from the Larmor frequency, the parameters which determine the relaxation rate are: correlation times τ_S and τ_L, the interproton separation distance a, and the angle α between the interproton vector and long molecular axis. Woessner's expression will be used in the analysis of the isotropic and paranematic phases, where the order parameter is relatively small (<0.1).

In the nematic and smectic-A phases the rotation of molecules around the short axis is hindered by the orientational order. This effect has been taken into account by introducing spatially anisotropic averages of quadratic and quartic terms, $\langle \sin^2 \theta \rangle$ and $\langle \sin^4 \theta \rangle$, where θ denotes the time-varying angle between the long molecular axis and the local director [31–33]. They are expressed in terms of the orientational order parameters S and $\langle P_4 \rangle$ (see the Appendix). The relaxation rate depends also on the angle Δ between the director and magnetic field. In uniaxial liquid crystals the spectral densities $J_k(\omega)$, determining the spin-lattice relaxation rate, are usually calculated for the orientation of the director parallel to the magnetic field. If the director is turned away from the magnetic field, the spectral densities are functions of Δ and were calculated elsewhere [33,34]. Within the extended Woessner's theory, the relaxation rate increases up to a factor ~2—depending on the magnitude of the order parameter—as Δ changes from 0° to 90°.

In treating local molecular reorientations, we neglect the contribution of conformational changes, which are usually faster than the reorientations of the whole molecule. Their contribution is frequency independent and of minor importance in the frequency range under study.

(ii) *Molecular translational self-diffusion in bulk liquid crystals (SD)* promotes spin relaxation only by modulating dipole-dipole interactions between spins in neighboring molecules, i.e., intermolecular spin interactions. The characteristic time associated with this process, the diffusion jump time τ_D, is usually shorter than the inverse Larmor frequency. For a typical value of the diffusion coefficient $D=5 \times 10^{-11}$ m^2/s and mean square jump distance to the nearest neighbor position $\langle r^2 \rangle \sim 1$ nm^2, τ_D is $\langle r^2 \rangle / 6D = 3 \times 10^{-9}$ s. Translational self-diffusion in bulk liquid crystals belongs therefore among "fast molecular motions." Its contribution to the total relaxation rate $(T_1^{-1})_{SD}$ was calculated in the closed form for viscous isotropic liquids by Torrey [35], and extended numerically for the nematic and smectic-A phases by Zumer and Vilfan [36]. The main parameters needed to calculate the relaxation rate $(T_1^{-1})_{SD}$ are the mean jump time τ_D, the distance of closest approach between spins in neighboring molecules b and spin density n. The spin-lattice relaxation rate in the nematic phase is given to a good approximation by the analytical Torrey's expression divided by 1.4. It shows a weakly decreasing angular dependence as the director is turned away from the magnetic field. In the smectic-A phase the dependence is exactly the opposite one.

(iii) *Molecular translational self-diffusion in confined liquid crystals (SD+RMTD)* has a much more important role

than in bulk sample. Naturally, it modulates intermolecular spin interactions on a fast time scale similarly as in the bulk, but in addition it modulates also stronger intramolecular proton spin interactions when the director is not uniform in space [37,38]. In systems where the orientational order parameter S is different from zero, the spin interactions are not completely averaged out by local molecular reorientations. The residual intramolecular interactions are further modulated in time as a molecule travels along the bends and joints of enclosures adapting itself to the local director orientation. Such molecular reorientations mediated by translational displacements (RMTD) occur on a much slower time scale than SD [39,40]. Characteristic times for the reorientation of a molecule depend on the structure of the director field and, intermediately, on the confining matrix. The RMTD process is formally described by the probability density that a molecule is displaced by a distance **r** in a time interval t, and by the probability that it alters the orientation from Ω_i to Ω_f in that distance **r**. In the case of normal diffusion, the probability density for the displacement **r** in time t has the Gaussian form and can be analyzed in terms of modes with wave numbers q. The orientational autocorrelation function for the diffusion along a mode with wave number q decays then exponentially with the characteristic time $\tau_q = (Dq^2)^{-1}$. In order to calculate the spin-lattice relaxation rate $(T_1^{-1})_{RMTD}$, spectral densities $J_k(\omega)_{RMTD}$ of the orientational autocorrelation functions are needed. Spectral densities $J_k(\omega)_{RMTD}$ contain the Lorentzian-type contributions of all q modes, weighted by the orientational structure factor $Q(q)$ which depends on the structure of the director field in the porous matrix. $J_1(\omega)_{RMTD}$ can be thus expressed in the form of an integral over q in the interval between q_{min} and q_{max} as

$$J_1(\omega)_{RMTD} = \int_{q_{min}}^{q_{max}} Q(q) \frac{2\tau_q}{1 + \omega^2 \tau_q^2} dq. \qquad (1)$$

In random porous media with isotropic distribution of pores orientation $J_2(\omega)_{RMTD} = 4J_1(\omega)_{RMTD}$.

The proton spin relaxation induced by RMTD has been observed in many porous media. The relaxation rate $(T_1^{-1})_{RMTD}$ of water in protein solutions [39], in liquid crystals above T_{NI} [19], in polymers with prevailing reptation process [13], and in several other systems turned out to be proportional to the inverse square root of the Larmor frequency in the range between $\omega_{RMTDmin} = Dq_{min}^2$ and $\omega_{RMTD\,max} = Dq_{max}^2$. The theoretical background leading to such behavior is an equipartition of wave numbers, describing the surface orientation, in the range between q_{min} and q_{max}, i.e., $Q(q) = $ const. The relaxation rate induced by RMTD is then [19,39,40]

$$\left(\frac{1}{T_1} \right)_{RMTD} = A_{RMTD} \left\{ \frac{1}{\omega^{1/2}} \left[f\left(\frac{\omega_{RMTD\,max}}{\omega} \right) - f\left(\frac{\omega_{RMTDmin}}{\omega} \right) \right] \right.$$
$$\left. + \frac{4}{(2\omega)^{1/2}} \left[f\left(\frac{\omega_{RMTD\,max}}{2\omega} \right) - f\left(\frac{\omega_{RMTDmin}}{2\omega} \right) \right] \right\},$$
$$(2)$$

where

$$f(y) = \frac{1}{\pi}\left[\arctan(\sqrt{2y} + 1) + \arctan(\sqrt{2y} - 1) \right.$$
$$\left. - \operatorname{arctanh}\left(\frac{\sqrt{2y}}{y + 1} \right) \right]. \tag{3}$$

The prefactor A_{RMTD} depends on the residual dipole-dipole proton spin interaction (averaged by local molecular reorientations), on the microstructural features of the confined liquid crystal, and on the diffusion coefficient. The low frequency cutoff $\omega_{RMTDmin}$ determines the inflection point where $(T_1^{-1})_{RMTD}$ levels off into a frequency independent plateau. The corresponding $(\tau_q)_{max} = (\omega_{RMTDmin})^{-1}$ is the decay time of the orientational correlation function for the diffusion along the mode with wave number q_{min}, and characterizes the slowest decay of orientational correlation. A different dispersion regime occurs at frequencies above $\omega_{RMTD\,max}$ where the slope of the dispersion curve increases and becomes proportional to ω^{-2}. The shortest correlation time $(\tau_q)_{min}$ is related to the smallest possible displacements of molecules where a notable change in the orientation of the director is obtained.

Generally, however, the orientational structure factor is a complex function of the wave number. In some cases it can be approximated by the analytical form [39]

$$Q(q) = cq^{-\chi} + e, \tag{4}$$

where c and e are constants independent of the wave number q. The constant e can be neglected in the low frequency dispersion regime as it reflects the impact of the closest, local environment and is less important. By inserting Eq. (4) with $e = 0$ into Eq. (1) and using the expression $\tau_q = (Dq^2)^{-1}$, the spectral density $J_k(\omega)_{RMTD}$ is proportional to

$$J_k(\omega)_{RMTD} \propto \int_{q_{min}}^{q_{max}} \frac{2\tau_q q^{-\chi}}{1 + \omega^2 \tau_q^2} dq = \frac{2}{D} \int_{q_{min}}^{q_{max}} \frac{q^{2-\chi}}{q^4 + \left(\frac{\omega}{D}\right)^2} dq. \tag{5}$$

Replacing $q\sqrt{D/\omega}$ by z yields

$$\left(\frac{1}{T_1}\right)_{RMTD} = A_{RMTD}\left\{ \frac{1}{\omega^p} \int_{z_{min}}^{z_{max}} \frac{z^{3-2p}}{1 + z^4} dz \right.$$
$$\left. + \text{the term at double } \omega \right\} \tag{6}$$

with $p = (1 + \chi)/2$, $z_{max} = (\omega_{RMTD\,max}/\omega)^{1/2}$, $z_{min} = (\omega_{RMTD\,min}/\omega)^{1/2}$. It should be noted that Eq. (2) is a special case of Eq. (6) when the orientational structure factor is constant ($\chi = 0$) and the result can be written in a closed form. The integration in Eq. (6) can be performed analytically for $\chi \neq 0$ by extending the limits of integration from zero to infinity. The resulting $(T_1^{-1})_{RMTD}$ dispersion curve is directly related to χ and follows the power law, $(T_1^{-1})_{RMTD} \propto \omega^{-(1+\chi)/2}$.

(iv) *Order director fluctuations (ODF)* are collective molecular orientational fluctuations of the director **n** relative to its time-averaged orientation. They are characterized by a broad frequency distribution of thermally activated modes which depend on the viscoelastic properties of the liquid crystal. The mean square amplitude of the splay-bend eigenmode and its relaxation time in the *nematic phase* are given by [41]

$$\langle |n_1(\mathbf{q})|^2 \rangle = \frac{k_B T}{V(K_1 q_\perp^2 + K_3 q_z^2)},$$

$$\tau(\mathbf{q}) = \frac{\eta_1}{K_1 q_\perp^2 + K_3 q_z^2}, \tag{7}$$

where K_1 and K_3 are the splay and bend elastic constants, respectively, V is the volume, and η_1 the effective viscosity; $q_\perp$ denotes the component of the wave vector perpendicular to the director and q_z is the component parallel to the director. Similarly, the twist-bend eigenmode is described as

$$\langle |n_2(\mathbf{q})|^2 \rangle = \frac{k_B T}{V(K_2 q_\perp^2 + K_3 q_z^2)},$$

$$\tau(\mathbf{q}) = \frac{\eta_2}{K_2 q_\perp^2 + K_3 q_z^2}, \tag{8}$$

where K_2 stands for the twist elastic constant. The spectral density $J_1(\omega)_{ODF}$ is the sum of contributions of all modes, converted into an integral in the limits from q_{min} to q_{max}. In denoting the wave vectors q and their limiting values q_{min} and q_{max}, we omit for the sake of simplicity the subscript ODF. It is understood that in the previous subsection (iii) the symbols q, q_{min}, and q_{max} referred to the translational diffusion modes, whereas here they denote the wave vectors of director fluctuations. For simplicity, the one-constant approximation with $K = K_1 = K_2 = K_3$ and $\eta = \eta_1 = \eta_2$ is used. The number of modes between q and dq in the isotropic three-dimensional space is given by the product $V/(2\pi)^3 4\pi q^2 dq$, and the spectral density $J_1(\omega)_{ODF}$ for the bulk nematic phase by

$$J_1(\omega)_{ODF} = \frac{V}{(2\pi)^3} \int_{q_{min}}^{q_{max}} \frac{k_B T}{VKq^2} \times \frac{\tau(q)}{1 + \omega^2 \tau^2(q)} 4\pi q^2 dq. \tag{9}$$

It should be mentioned that in deriving Eq. (9), the theory is restricted to the harmonic regime of small fluctuations. Consequently, only the spectral density of the correlation function which is quadratic in the displacement angle $J_1(\omega)_{ODF}$ is retained, whereas $J_2(\omega)_{ODF} \simeq 0$. In the frame with director parallel to the magnetic field, $(T_1^{-1})_{ODF}$ of a proton pair is then [42]

$$\left(\frac{1}{T_1}\right)_{ODF} = \frac{A_{ODF}}{\omega^{1/2}}\left[f\left(\frac{\omega_{ODF\,max}}{\omega}\right) - f\left(\frac{\omega_{ODF\,min}}{\omega}\right) \right], \tag{10}$$

with

$$A_{ODF} = \frac{9}{8} \left(\frac{\mu_0}{4\pi} \right)^2 \frac{\gamma^4 \hbar^2}{a_{eff}^6} \frac{k_B T S^2 \eta^{1/2}}{\sqrt{2} \pi K^{3/2}}, \qquad (11)$$

where $f(\omega_{ODF\,max}/\omega)$ and $f(\omega_{ODF\,min}/\omega)$ are given by Eq. (3), and $(\mu_0/4\pi)^2 S^2 \gamma^4 \hbar^2/a_{eff}^6$ denotes the effective residual strength of dipolar interaction. The factor a_{eff}^{-6} stands for the expression $a^{-6}(3\cos^2\alpha - 1)^2/4$ where a denotes the interproton distance and α the angle between the interproton vector and long molecular axis. S is the order parameter related to the deviations of the long molecular axis from the local director. The cutoff frequencies $\omega_{ODF\,max} = Kq_{max}^2/\eta$ and $\omega_{ODF\,min} = Kq_{min}^2/\eta$ are the limits of the frequency range where the spin-lattice relaxation follows the well known power law $(T_1^{-1})_{ODF} \propto \omega^{-1/2}$. A similar frequency dependence appears also in the *isotropic phase just above the transition point*. It is ascribed to the fluctuations in the degree of orientational order and denoted as $(T_1^{-1})_{OF}$. The corresponding A_{OF} is smaller than in the nematic phase. It should be stressed that the origin of the inverse square root frequency dispersion in the case of ODF or OF [Eq. (10)] is different from that of the RMTD [Eq. (2)]. In the former case, the increasing number of modes with larger q is compensated by their smaller mean square amplitude and is valid generally for the nematic phase. At variance, in treating RMTD an equipartition of different q modes is assumed as a special case of the orientational structure factor.

In the *smectic-A phase*, director fluctuations have less freedom than in the nematic phase. The layered structure imposes severe constraints on the twist and bend elastic deformations. Energetically least expensive are *layer undulations (LUs)*, which are pure splay deformations and spread only in two dimensions, i.e., in the plane of the layer. The corresponding spin-lattice relaxation rate is [42,43]

$$\left(\frac{1}{T_1} \right)_{LU} = \frac{A_{LU}}{\omega \pi} \left[\arctan\left(\frac{\omega_{ODF\,max}}{\omega} \right) - \arctan\left(\frac{\omega_{ODF\,min}}{\omega} \right) \right], \qquad (12)$$

with

$$A_{LU} = \frac{9}{16} \left(\frac{\mu_0}{4\pi} \right)^2 \frac{\gamma^4 \hbar^2}{a_{eff}^6} \frac{k_B T S^2}{L K_1}, \qquad (13)$$

where L is the correlation length of undulations.

The magnitude of $(T_1^{-1})_{ODF}$ and $(T_1^{-1})_{LU}$ increases somewhat as the director is turned away from the magnetic field. The angular dependence must be taken into account if the liquid crystal is confined into a matrix with randomly oriented local pore segments. This is, however, only the minor *effect of the confinement*. The most important difference arises from the fact that the wavelengths of fluctuations perpendicular to the long axis of the pore segment are limited by the transverse size of the cavity. The spectrum of normal modes $q_\perp$ is here discrete in contrast to the bulk where the fluctuations are expressed in terms of waves with a continous distribution of wave vectors. In the strong anchoring approach, the orientation of director is fixed at the glassy surface, so the fluctuations vanish there. The smallest allowed $q_\perp$ is of the order $\pi/2R$, where $2R$ denotes the diameter of

the cavity. The absence of smaller $q_\perp$ values has a profound diminishing effect on the magnitude of $(T_1^{-1})_{ODF}$. The $\omega^{-1/2}$ dispersion regime becomes narrower and levels off at a higher $\omega_{ODF\,min}$ than in the bulk [44]. Notably, the restriction in one dimension is sufficient to provoke the effect of confinement and decrease the relaxation rate.

In confined liquid crystals it might happen that a fractal dimensionality governs the fluctuations of the director in some special cases [18]. In a fractal system with dimensionality d, the number of q modes between q and $q+dq$ must be calculated anew. Taking into account that the surface of a hypersphere of dimensionality d is $\pi^{d/2} dq^{d-1}/\Gamma(d/2+1)$, the number of q modes between q and $q+dq$ is [18]

$$\left(\frac{L}{2\pi} \right)^d \pi^{d/2} \frac{dq^{d-1}}{\Gamma(d/2+1)} dq. \qquad (14)$$

This expression includes the Gamma function Γ [45] and the size L of the fractal domain where dynamical correlations occur. For $d=3$, it reduces to the well known product $V/(2\pi)^3 4\pi q^2 dq$, which has been used in deriving Eqs. (10) and (11). By replacing the three-dimensional density of q modes in Eq. (9) by Eq. (14) and integrating over q from zero to infinity, the spin-lattice relaxation rate due to order director fluctuations in a general, d-dimensional space is obtained:

$$\left(\frac{1}{T_1} \right)_{ODF-d} = \frac{9}{2^{d+2}} \frac{\pi^{1-d/2}}{\Gamma(d/2)\sin(d\pi/4)}$$
$$\times \left(\frac{\mu_0}{4\pi} \right)^2 \frac{\gamma^4 \hbar^2}{a_{eff}^6} \frac{k_B T S^2 \eta^{d/2-1}}{K^{d/2} L^{3-d}} \frac{1}{\omega^{2-d/2}}. \qquad (15)$$

The main feature of Eq. (15) worth stressing is the specific power-law dependence of the relaxation rate on the Larmor frequency, i.e., $(T_1^{-1})_{ODF-d} \propto \omega^{d/2-2}$. Other relevant quantities that enter as dimension-dependent parameters are the elastic constant, viscosity, and the size of the region with correlated fluctuations. It is interesting to note that the dependence of relaxation rate on the correlation length vanishes only in the three-dimensional case, e.g., in the bulk nematic phase. Similarly, in two-dimensional systems the effect of viscosity is absent. It should be stressed that Eq. (15) matches exactly the relaxation rates calculated earlier for the three-, two-, and one-dimensional systems if one takes into account that in the strictly described smectic-A phase the twist-bend mode is not allowed, and that in a one-dimensional system only the bend mode is considered [42]. Though expressed in terms of partly different parameters, Eq. (15) of the present paper is generally in agreement with Eq. (4) of Ref. [18] (see comment [46]).

IV. ANALYSIS OF T_1^{-1} DISPERSIONS AND DISCUSSION

The dispersions of spin-lattice relaxation over a broad frequency range reveal dynamic processes in various phases of the system. As discussed previously, in liquid crystals, and particularly in nanoconfined liquid crystals, the spin-lattice relaxation is not the result of a simple process. It is composed of contributions of several relaxation mechanisms: fast
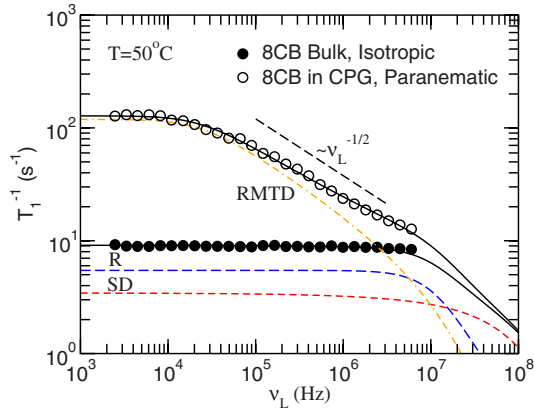
FIG. 4. (Color online) Frequency dependence of the proton spin-lattice relaxation rate T_1^{-1} of 8CB in the bulk (solid circles) and of 8CB confined into porous glass CPG (open circles) at 50 °C. The solid lines, representing the calculated total relaxation rates, were obtained by fitting Eq. (16) to the experimental data. The relaxation mechanisms involved are local molecular reorientations (R), translational self-diffusion (SD), and slow reorientations mediated by translational displacements (RMTD). The solid line through the bulk data is the sum of R and SD contributions, whereas the solid line through the data of the nanoconfined sample includes also the RMTD contribution. The fitted values of free parameters are listed in Table I.

local molecular motions and slower reorientations, induced either by translational displacements or director fluctuations. The total relaxation rate is the sum of contributions of different dynamic processes [8,47]:

$$\left(\frac{1}{T_1}\right) = \left(\frac{1}{T_1}\right)_R + \left(\frac{1}{T_1}\right)_{SD} + \left(\frac{1}{T_1}\right)_{RMTD} + \left(\frac{1}{T_1}\right)_{ODF}. \quad (16)$$

Apart from the RMTD contribution, which enters only in the nanoconfined sample, the other three relaxation mechanisms are present in bulk as well as in the porous glass though their contributions might be modified by the confinement. When fitting experimental data to the theoretical expressions it is important to take into account all relaxation mechanisms. Omitting fast molecular motions, for example, might give misleading results for the power-law exponent of the relaxation rate induced by slow motions, etc.

To get a quantitative insight into the spin-lattice relaxation process, we fit Eq. (16)—with details given in Sec. III and in the Appendix—to the experimental data. The analysis is performed by the nonlinear least-square fitting minimization procedure. The fitted parameters are (i) the correlation time for the reorientations around the short molecular axis τ_S, (ii) the strength of director fluctuations A_{ODF} (replaced by A_{OF} above T_{NI}), (iii) their low-frequency cutoff ω_{ODFmin}, (iv) the strength of the RMTD mechanism A_{RMTD} and its exponent p, (v) the low- and high-frequency cutoffs $\omega_{RMTD\,min}$ and $\omega_{RMTD\,max}$. The fitted values of the free parameters used in calculating the dispersion curves in Figs. 4–7 are presented in Table I.

It should be mentioned that in order to simplify the fitting procedure, we fixed those parameters which have well
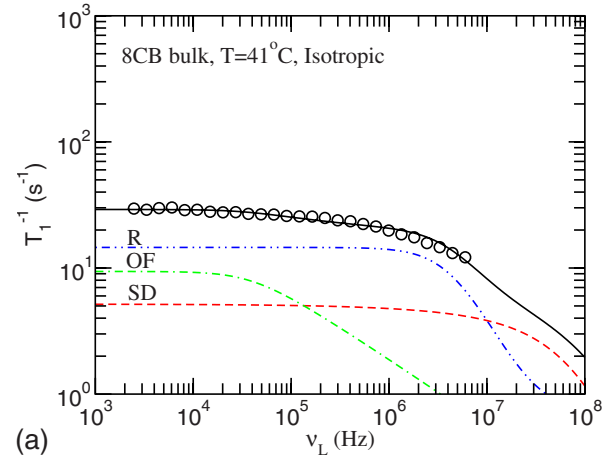
(a)
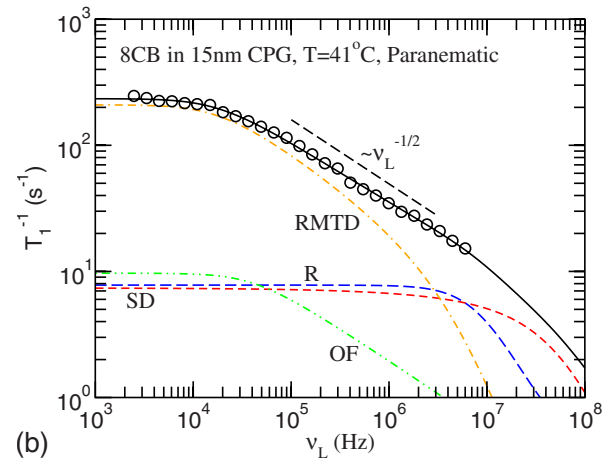
(b)

FIG. 5. (Color online) Frequency dispersion of the proton spin-lattice relaxation rate T_1^{-1} of 8CB at 41 °C: (a) in the bulk, and (b) confined into porous glass CPG. 8CB at 41 °C is isotropic in the bulk and paranematic in the nanoconfined state. The solid line, representing the calculated total relaxation rate, was obtained by fitting Eq. (16) to the experimental data (details are given in the text). The relaxation mechanisms involved are local molecular reorientations (R), translational self-diffusion (SD), order fluctuations (OF), and slow reorientations mediated by translational displacements (RMTD). The fitted values of free parameters are given in Table I.

known values from other studies. The prefactor related to the effective strength of dipolar interactions A_{ROT} and the distance of closest approach of spins in neighboring molecules b have fixed values determined from the fit in the bulk nematic phase at 37 °C, where the shape of the dispersion curve allows for the best accuracy. The mean jump time τ_D, characteristic of translational diffusion, has been calculated using the bulk diffusion coefficient D at different temperatures (taken from Ref. [48]). Recent deuteron NMR studies namely indicate that local D has roughly the same value in the confined state as in the bulk [27]. In the isotropic phase $\tau_D = \langle r^2 \rangle / (6D)$; in the ordered phases, its component perpendicular to the director, $\tau_{D\perp} = \langle r_\perp^2 \rangle / (4D_\perp)$, enters into the theoretical expressions of Ref. [36]. The proton spin density n $= 5.17 \times 10^{28}$ per m^3 has been calculated from the density of
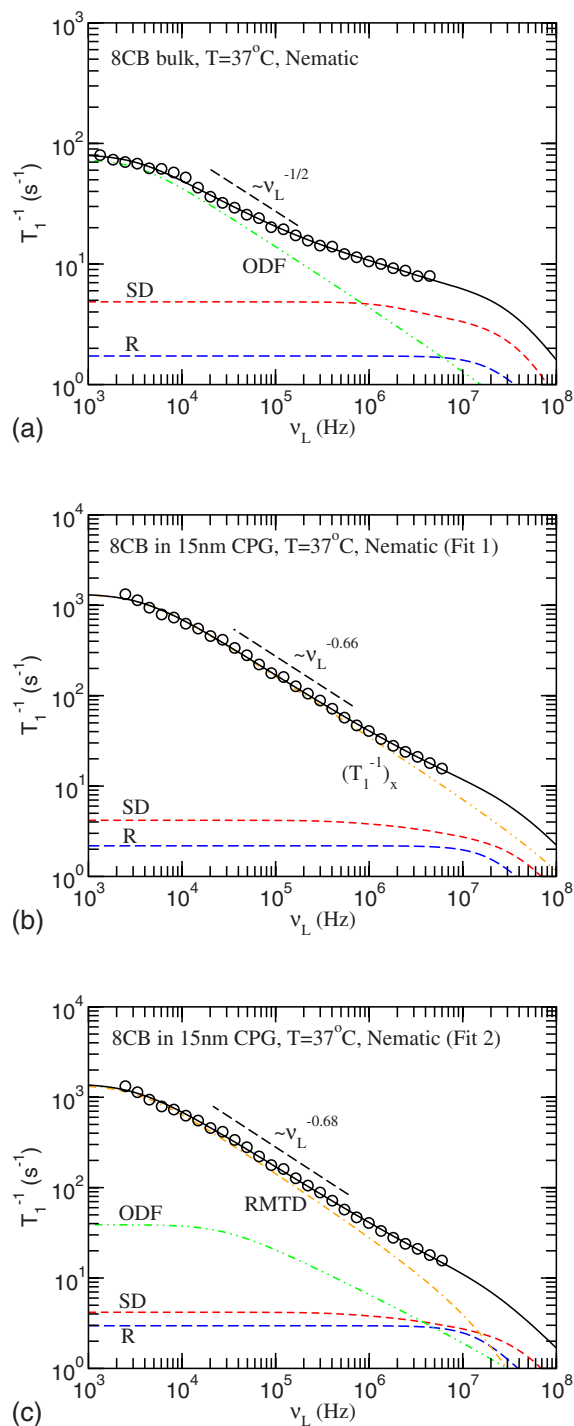
FIG. 6. (Color online) Frequency dispersions of the proton spin-lattice relaxation rate T_1^{-1} of nematic 8CB at 37 °C: (a) in the bulk, (b) confined into porous glass CPG (fit 1), and (c) confined into porous glass CPG (fit 2). In fit 1 the experimental data are explained by a superposition of three relaxation mechanisms: molecular reorientations (R), translational self-diffusion (SD), and a power-law contribution $(T_1^{-1})_x$. In fit 2, $(T_1^{-1})_x$ is replaced by the sum of separate contributions of reorientations mediated by translational displacements (RMTD) and order director fluctuations (ODFs). The solid line represents the sum of the contributions of all relaxation mechanisms. The fitted values of the free parameters are given in Table I.

8CB. It was further assumed that the mean square jump distance is $\simeq b^2$, and that the ratio τ_S/τ_L equals 10 in the isotropic phase and 5 in the nematic and smectic-A phases. This assumption is not problematic as the last two parameters ($\langle r^2 \rangle/b^2$ and τ_S/τ_L) have hardly any impact on the results of the fit. Similarly, $\omega_{ODF\ max}$ is fixed to $2\pi \times 10^9$ Hz, its effect being out of the frequency range of our study. A few material parameters which enter into the theoretical expressions for R are listed in the Appendix.

A. Spin-lattice relaxation above the bulk T_{NI}

T_1^{-1} experimental data obtained for the nanoconfined 8CB at 50 °C correspond to the paranematic phase with a thin ordered layer next to the surface and disordered central part of the cavity. Closer to the phase transition, at 41 °C, the nematic correlation length is large enough to spread a weak orientational order throughout the cavity, though the magnitude of the order parameter decays from the surface towards the centre of the pore. In Figs. 4 and 5, the T_1^{-1} dispersions for the nanoconfined and bulk 8CB above T_{NI} are presented. The inspection shows a huge increase in the relaxation rate upon confinement. Actually, at Larmor frequency ~ 10 kHz the relaxation rate in CPG is more than ten times larger than in the bulk. The T_1^{-1} dispersions are also qualitatively different. The relaxation rate in the bulk does not show any frequency dependence at 50 °C and only a weak one at 41 °C. On the other hand, T_1^{-1} of the nanoconfined 8CB displays a well expressed power-law dispersion with a plateau below the low frequency cutoff.

The spin-lattice relaxation in the bulk 8CB at 50 °C is well described by a superposition of two relaxation mechanisms: local molecular reorientations (R) and molecular translational self-diffusion (SD) (Fig. 4). The correlation times of these dynamic processes are smaller than the inverse Larmor frequency. The fitted value of the correlation time related to the reorientations around the short molecular axis, $\tau_S \sim 7 \times 10^{-9}$ s, is in good agreement with the results of dielectric measurements [6,26]. At 41 °C [Fig. 5(a)], a better fit of Eq. (16) to the experimental data is obtainded if—in addition to R and SD—the $(T_1^{-1})_{OF}$ contribution is taken into account. It arises from the formation and decay of small nematic clusters within the isotropic phase. The onset of an additional relaxational mechanism is clearly indicated by the slope of the experimental T_1^{-1} dispersion curve in the range between $\sim 3 \times 10^4$ and 10^6 Hz. Though small, the slope is definitely different from zero. No frequency dependence in this range can be observed at 50 °C.

Figures 4 and 5(b) show that the large T_1^{-1} of the nanoconfined 8CB can be consistently explained by a sum of the RMTD-induced relaxation rate, described by Eq. (2), and the bulklike contributions of other molecular motions. Obviously, RMTD is the most effective relaxation mechanism below ~ 10 MHz. Between the two cutoffs it exhibits the characteristic power-law frequency dependence $(T_1^{-1})_{RMTD} \propto \omega^{-1/2}$, which means that we deal with an equipartition of diffusion modes with different wavelengths. The fitted cutoff frequencies $\omega_{RMTD\ min}$ and $\omega_{RMTD\ max}$ are related to the largest

TABLE I. The best fit values of parameters used in calculating the dispersion curves presented in Figs. 4–7. A_{ROT} and b have been determined in the fit of the bulk nematic phase, where the shape of the dispersion curve allows for the best accuracy, and fixed elsewhere. A_x, the corresponding cutoff frequencies, and p refer to the fits of the nanoconfined 8CB at 37 °C (fit 1) and at 28 °C, where a single relaxation rate contribution $(T_1^{-1})_x$, comprising both RMTD and ODF, is assumed.

	8CB bulk			8CB in 15 nm CPG				
Phase	I	I	N	P	P	N (fit 1)	N (fit 2)	$N \to$ Sm-A
T (°C)	50	41	37	50	41	37	37	28
τ_s (10^{-9} s)	6.9	17	3.1	6.7	3.7	3.1	4.2	10
A_{ROT} (10^{10} s^{-2})		8.82				8.82		
τ_D, $\tau_{D_\perp}$ (10^{-10} s) (calculated)	7.0	10	17	7.0	10	17	17	26
b (10^{-10} m)		4				4		
A_{ODF}, A_{OF} (10^3 s$^{-3/2}$)		4.8	11	5.0			11	
$\omega_{ODFmin}/2\pi$ (10^3 Hz)		34	2.9	34			42	
$\omega_{ODFmax}/2\pi$ (10^9 Hz) (calculated)		1.0	1.0	1.0			1.0	
A_{RMTD}, A_x (10^5 s$^{-(1+p)}$)				0.13	0.20	3.8	4.2	76
$\omega_{RMTDmin}/2\pi$ (10^3 Hz)				35	26	5.5	4.8	7.2
$\omega_{RMTDmax}/2\pi$ (10^7 Hz)				4.0	1.0	74	5.1	10
p				0.5	0.5	0.66	0.68	0.86

and smallest molecular displacements, ℓ_{max} and ℓ_{min}, respectively, between positions which impose uncorrelated orientations. An estimate of the ℓ_{max} and ℓ_{min}, however, depends on the model, i.e., on the dimensionality of the diffusion which induces relaxation-relevant displacements. Assuming a topologically two-dimensional curvilinear displacement along the surface, $(\omega_{RMTD\,min})^{-1} = (\tau_q)_{max} \simeq \ell_{max}^2/4D$ and $(\omega_{RMTD\,max})^{-1} = (\tau_q)_{min} \simeq \ell_{min}^2/4D$. For $D = 6 \times 10^{-11}$ m^2/s at 50 °C [48], we find $\ell_{max} \simeq 33$ nm, which is only about twice the diameter of the cavity. The smaller distance ℓ_{min} is of the order of molecular size and suggests a nonuniform arrangement on the local scale, most probably a random planar ordering at the surface. It is interesting to note that the displacement ℓ_{max} in the paranematic phase shows hardly any variation with temperature. The decrease in $\omega_{RMTDmin}$ from $2\pi \times 35$ kHz at 50 °C to $2\pi \times 26$ kHz at 41 °C comes entirely from the decrease in the diffusion coefficient. The fitted value for τ_S at 50 °C is nearly the same as in the bulk. Closer to the phase transition, at 41 °C, τ_S in CPG is somewhat shorter than in the bulk, indicating that the orientational order—extending at this temperature over the whole cavity—reduces the amplitude of reorientations around the short molecular axis.

One might argue that the RMTD contribution in the confined 8CB might be—in view of its inverse square root dependence on the Larmor frequency—explained alternatively by an increase in the order fluctuation (OF) relaxation rate. There are, however, two arguments against this conjecture. First, the decay time of nematic clusters is slightly shorter in the confined isotropic phase than in the bulk [49] and cannot provide an increase in the OF relaxation rate at low frequencies. Second, possible fluctuations in the thickness of the surface layer differ from the bulk fluctuations only in a small temperature interval of about 1 K above T_{NI} [10]. Obviously,

they cannot account for the increase in T_1^{-1} which is well expressed 10 K and more above the bulk transition temperature.

B. Nematic phase

Upon cooling the samples into the nematic phase, a strong increase in the spin-lattice relaxation rate at low frequencies is observed both in the bulk and in the nanoconfined 8CB. It stems from the onset of the long-range orientational order. In Fig. 6(a) the bulk nematic data are presented and the well-known dispersion of director fluctuations (ODFs) is clearly seen. The contribution of translational diffusion (SD) is almost the same as in the isotropic phase, whereas the part of local reorientations (R) is smaller in view of shorter correlation time of hindered rotations around the short molecular axis. Comparing Fig. 6(a) with Figs. 6(b) and 6(c), one can see that—similarly as in the isotropic phase—the confinement drastically increases the relaxation rate. Again, the observed T_1^{-1} for the nematic phase of 8CB in porous glass is about ten times larger than in the bulk at ~ 1 kHz.

In the first step we do not specify the origin of the relaxation mechanism responsible for this increase. We denote its contribution to the total relaxation rate by $(T_1^{-1})_x$ and assume that it has the general form of a power-law dispersion with exponent p, i.e., $(T_1^{-1})_x \propto \omega^{-p}$, in the range between the low- and high-frequency cutoffs. Figure 6(b) (fit 1) shows that the T_1^{-1} data of nanoconfined 8CB in the nematic phase can be straightforwardly fitted by $(T_1^{-1})_x$ superimposed on the standard contributions of local reorientations and self-diffusion. It turns out that the parameters describing the R and SD contributions are almost identical to those in the bulk (see

Table I). The magnitude of their contributions, however, is not the same as they depend on the angle between the director and magnetic field. We took into account that in the bulk nematic phase the director is everywhere parallel to the magnetic field while it adjusts itself to the random orientation of pore segments in the glass. In calculating the relaxation rates in the confined nematic phase an isotropic distribution of director orientations was assumed. The prefactors of spectral densities were calculated by averaging the terms with $\sin^2 \Delta$ and $\sin^4 \Delta$ over all director orientations [33,34].

In the following, the origin of the $(T_1^{-1})_x$ is discussed. The best fit value of the exponent p related to $(T_1^{-1})_x$ is 0.66 ± 0.01. At first sight, it might be tempting to ascribe the power-law dispersion curve with exponent 0.66 to order director fluctuations in a fractal medium. Namely, the exponent changes according to the dimensionality of the system, $p = 2 - d/2$, where d denotes the dimensionality [see Eq. (15)]. A good test whether the dimensionality $d = 2.68$, obtained from $p = 0.66$, explains reasonably well the experimental data is the value of the correlation length L calculated from Eq. (15). Using $(T_1^{-1})_x = 800$ s^{-1} at $\omega = 2\pi \times 10^4$ Hz, $(\mu_0/4\pi)^2 (\gamma^4 \hbar^2 / a_{eff}^6) S^2 \simeq 3.8 \times 10^9$ s^{-2} (extracted from the bulk ODF contribution), $d = 2.68$ (from the fit), viscosity $\eta = 0.056$ N s m^{-2} [50], and $K = 2 \times 10^{-11}$ N [51], it turns out that L is only 1.7×10^{-11} m. This result does not make sense as the correlation length of director fluctuations—which are a collective process—should extend over many molecular lengths. Taking into account a random distribution of director orientations, L of the same order of magnitude is obtained. The possibility that ODF in the fractal medium is the leading relaxation mechanism is thus completely discarded. Moreover, the same argument applies not only to 8CB in CPG with 15 nm pores but also to other strongly confined liquid crystalline systems. For example, taking the experimental data and parameters from Ref. [18] and inserting them into Eq. (4) of the same paper, a correlation length $L \sim 0.4$ nm is obtained which is by far too small to justify the leading role of collective orientational fluctuations in the spin relaxation process.

Consequently, it is more reasonable to assume that $(T_1^{-1})_x$ originates from director fluctuations only to a smaller extent. The spatial confinement imposes restrictions on the ODF modes. If one assumes a strictly strong anchoring of liquid crystal molecules at the glassy wall, only the modes with wavelength smaller than $\sim 4R \simeq 30$ nm in the plane perpendicular to the molecular director are allowed. In such a case, the low-frequency cutoff for $(T_1^{-1})_{ODF}$ is about $\omega_{ODF\ min} = K(2\pi)^2/(\eta \lambda_{max}^2) \simeq 15 \times 10^6$ Hz. The corresponding $(T_1^{-1})_{ODF}$ value is relatively small (~ 5 s^{-1}) and frequency independent in the whole kilohertz range. Obviously, the confinement reduces the ODF contribution. It is consequently expected that RMTD would represent the major part of $(T_1^{-1})_x$. In order to calculate the magnitude of the RMTD contribution, the orientational structure factor of the CPG system should be known but it is not. Still, a rough estimate can be made by replacing the q-dependent "distribution" of diffusion times by a single characteristic time τ_{RMTD}. In the low frequency limit the "plateau" value of $(T_1^{-1})_{RMTD}$ in this simplified form is [19,38]
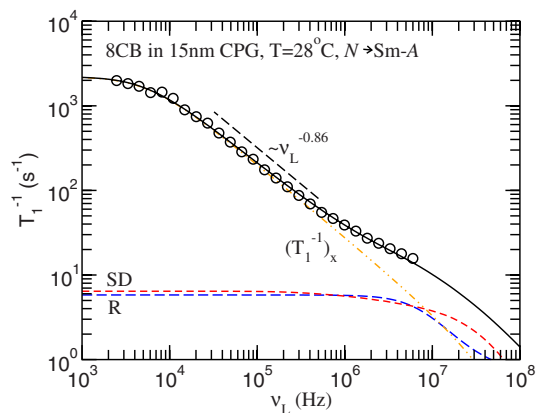
FIG. 7. (Color online) Frequency dispersions of the proton spin-lattice relaxation rate T_1^{-1} of 8CB confined into porous glass CPG at 28 °C, where the transition to the smectic-A phase is occuring. The experimental data are explained by a superposition of three relaxation mechanisms: molecular reorientations (R), translational self-diffusion (SD), and a power-law contribution $(T_1^{-1})_x$. The solid line represents the sum of the three contributions. The fitted values of the free parameters are given in Table I.

$$\left(\frac{1}{T_1} \right)_{RMTD} \sim \frac{3}{2} \left(\frac{\mu_0}{4\pi} \right)^2 \frac{\gamma^4 \hbar^2}{a_{eff}^6} S^2 \tau_{RMTD}. \qquad (17)$$

Using $(T_1^{-1})_{RMTD} \sim 1300$ s^{-1} and $(\mu_0/4\pi)^2 S^2 \gamma^4 \hbar^2 / a_{eff}^6 \simeq 3.8 \times 10^9$ s^{-2}, one obtains an effective $\tau_{RMTD} \sim 2.3 \times 10^{-7}$ s. The distance traveled in this time by a molecule is of the order of 10 nm. Though the above approximation is extremely rough it shows at least that the RMTD mechanism is perfectly capable to account for the large relaxation rate in the nanoconfined system.

To summarize, RMTD is the prevailing relaxation mechanism responsible for the large T_1^{-1} in the nanoconfined nematic phase. The parameters obtained for $(T_1^{-1})_x$ can be for all practical purposes considered as the parameters describing RMTD. Still, in the next step we perform an additional fit (fit 2), where $(T_1^{-1})_x$ is replaced by $(T_1^{-1})_{ODF} + (T_1^{-1})_{RMTD}$ [Eqs. (10) and (6), respectively] in order to get a quantitative notion of the separate ODF and RMTD contributions. The low frequency cutoff of ODF is left as a free parameter whereas the prefactor A_{ODF} is fixed to the bulk value (a possibly smaller S in the confined state would be compensated by a correlated change in K and η, and would not affect A_{ODF}). The result of this fit is presented in Fig. 6(c). As expected, RMTD turns out to be the main relaxation mechanism. Its characteristic exponent $p = 0.68 \pm 0.01$ is nearly the same as in fit 1 and obviously stable against reasonable variations in the magnitude of the ODF contribution. The exponent p is larger than in the paranematic phase and steadily increases on cooling the sample in the nematic phase; for example, it is as big as $\sim 0.78 \pm 0.01$ already at 34 °C. The value of p above 0.5 means that the equipartition of diffusion modes does not hold any more. The relative importance of diffusion modes with larger wavelengths has increased. This can be interpreted as a natural consequence of the more uniform orientation of the director within one pore segment in the

nematic phase than in the paranematic. Actually, it corresponds to a transition from the random planar to the uniform planar surface arrangement of molecules.

The fitted value for the low-frequency cutoff $\omega_{RMTD\,min} \simeq 2\pi \times 4.8$ kHz is above the effect of local field and represents an intrinsic parameter of the system. It is related to the largest diffusion time $(\tau_q)_{max} = (\omega_{RMTDmin})^{-1} \simeq 3.3 \times 10^{-5}$ s during which the orientational correlation is lost in the RMTD process. In this time a molecule travels in the direction along the pore the distance $\ell_{max} = \sqrt{2D_{\parallel}(\tau_q)_{max}} \simeq 60$ nm which is comparable to the estimated length of a pore segment (we used $D_{\parallel} \simeq 5 \times 10^{-11}$ m^2/s [48]).

Though the ODF contribution in fit 2 is less important, it deserves a few words of comment. The fitted value for $\omega_{ODF\,min} \simeq 2\pi \times 42$ kHz is smaller than the one calculated for the strong anchoring limit. The corresponding maximum wavelength of director fluctuations perpendicular to the pore axis is effectively larger than the diameter of the pore, $\lambda_{ODF\,max} = \sqrt{4\pi^2 K / \eta \omega_{ODF\,min}} \sim 230$ nm. Obviously, in the case of 8CB in CPG the limit of strong surface anchoring is not fulfilled in the nematic phase. It is further interesting to note that the decay time of slowest director fluctuations, $\tau_{ODF\,max} = (\omega_{ODFmin})^{-1} \sim 3.8 \times 10^{-6}$ s, is about ten times shorter than the time required for a molecule to diffuse over ℓ_{max} of the RMTD process. This fact shows that treating RMTD and ODF separately is roughly justified only below $\sim 10^5$ Hz; above this frequency, the characteristic times of the two dynamic processes, i.e., the times which are most effective in the spin relaxation at a fixed frequency, are partly overlapping and their interplay should not be neglected. For this reason the values obtained in fit 2 for the high-frequency cutoff of RMTD are not reliable.

C. Transition into the smectic-*A* phase

In the bulk 8CB the transition from the nematic into the smectic-*A* phase is of the second order. Though the orientational order parameter does not experience a discontinous jump, the transition is well marked by a discontinous drop in the relaxation rate [Fig. 2(a)], and by a big change in the shape of the dispersion curves [Fig. 3(a)]. The layered structure obviously reduces the effectiveness of director fluctuations. At variance, the diffusion coefficient decreases continously through the nematic-smectic-*A* transition. A complete lack of any significant change in T_1^{-1} of the nanoconfined 8CB at this temperature strongly supports the scenario with RMTD acting as the main relaxation mechanism. Actually, at 28 °C, where other techniques reveal at least a partial onset of the smectic-*A* phase, the proton T_1^{-1} exhibits—in addition to the standard SD and *R* contributions—a power-law dispersion similar to that in the nematic phase (Fig. 7). There is a moderate increase in the exponent, $p = 0.86 \pm 0.03$, suggesting that within the interval between q_{min} and q_{max} the modes with relatively longer wavelengths are taking over the relaxation process. On the other hand, the low-frequency cutoff is somewhat larger than in the nematic phase, $\omega_{RMTD\,min} \sim 2\pi \times 7.2$ kHz, leading to a smaller ℓ_{max} when $D_{\parallel} \simeq 3 \times 10^{-11}$ m^2/s is taken into account [48]. The origin of a smaller ℓ_{max} with respect to the nematic phase is not clear. It may be the sign that the variations in the orientation of the director or in the magnitude of the order parameter occur on a smaller distance. The incoming smectic-*A* structure is obviously strongly perturbed and the complexity of the system has increased due to the short range regions with smectic order.

The fit presented in Fig. 7 can be further improved by allowing separately for the contributions of RMTD and director fluctuations. It turns out that the ODF contribution—though much smaller than that of RMTD—is better described by fluctuations of the nematic type. The low-frequency cutoff is $\sim 38 \times 10^6$ Hz which means that the strength of the surface anchoring has increased with decreasing temperature.

V. CONCLUSIONS

In this paper we present a proton spin-lattice relaxation study of liquid crystal 8CB confined into pores of the CPG glass with the average diameter ~ 15 nm. The data are compared with those of the bulk 8CB at temperatures corresponding to the isotropic, nematic and smectic-*A* phases. As expected, there is a drastic increase in the spin-lattice relaxation rate T_1^{-1} of the nanoconfined 8CB with respect to the bulk. The effect of the confinement increases with decreasing size of the enclosures. It is observable particularly in the kHz Larmor frequency range. For example, at 50 °C and Larmor frequency 10 kHz, the relaxation rate of 8CB is ~ 8 s^{-1} in the bulk and 120 s^{-1} in ~ 15 nm cavities. We show that the relaxation mechanism responsible for the increase upon confinement can be well described by a power-law dispersion in the frequency range between the low and high frequency cutoffs. It is reasonable to assume that this relaxation mechanism results from a combination of molecular reorientations modulated by translational displacements, RMTD, and collective order director fluctuations, ODF. RMTD should be here understood in a broad sense, i.e., it includes the modulation both of the molecular director and of the local order parameter (the latter is important particularly above T_{NI}). The analysis of experimental data shows that the major part of increase in T_1^{-1} is due to RMTD (more than 90% below ~ 100 kHz). There are also several qualitative arguments which corroborate the conclusion that the major increase in T_1^{-1} upon confinement is induced by RMTD as follows:

(i) A strong increase in the relaxation rate upon confinement is observed at 10 K and more above the nematic-isotropic phase transition. According to the work of Schwalb and Deeg [49], the relaxation time of order parameter fluctuations (OFs) above T_{NI} is reduced with respect to the bulk and does not diverge. For this reason the contribution of OF to the spin-lattice relaxation rate cannot be larger (more probably it is smaller) than in the bulk. On the other hand, RMTD of molecules in the ordered surface layer, which is not present in the bulk, adds to the relaxation rate.

(ii) In the nematic phase the confinement reduces the number of ODF modes and, consequently, its contribution to T_1^{-1}. The reduction is expressed in the dispersion curve as an increase in the low frequency cutoff.

(iii) The exponent p in the nematic phase is not ~0.5 as should be for the ODF mechanism but assumes different values between 0.65 and 0.9. One possibility to account for this change in the exponent and still stick to the ODF mechanism might be the fractal nature of the enclosures. In this case, however, the exponent would not change with temperature. Moreover, assuming that the director fluctuations in the fractal medium are the main relaxation mechanism, the correlation length calculated from experimental data is unreasonably small and discards this conjecture.

(iv) The relaxation rate is steadily increasing in the temperature range where the smectic order starts to appear. There is no decrease in T_1^{-1}, which would be expected on the basis of the bulk data if ODF would be the dominant relaxation mechanism.

(v) A simplified calculation of the RMTD contribution shows that it is perfectly capable to account for the observed large increase in T_1^{-1} upon confinement.

Taking into account these arguments we could explain the measured data as a superposition of two fast and two slow relaxation mechanisms in the NMR time scale. The former two include local molecular reorientations with the correlation time for rotations around the short molecular axis in the range between 10^{-9} and 10^{-8} s, and bulklike translational self-diffusion acting intermolecularly. Obviously, the confinement into ~15 nm pores does not significantly affect local rotational and translational dynamics of molecules. This observation is not in contradiction with the direct NMR measurements of the diffusion coefficient which reflect the tortuosity of the glassy matrix and not only local translational diffusion within one pore segment. It should be mentioned that omitting the contributions of fast motions in the analysis of T_1^{-1} data might lead to erroneous results for the slow dynamic processes.

RMTD is the slow relaxation mechanism responsible for the increase in the relaxation rate in confined liquid crystals. It is induced by molecular migration along the curvatures and crossroads of the pore segments implying that a molecule adjusts itself to the local director and order parameter. The RMTD dispersion curve is characterized by an exponent which reflects the structure of the director and order parameter field in the cavities. The characteristic exponent steadily varies with decreasing temperature. It is close to 0.5 in the high-temperature phase, 0.68 just below the transition into the nematic phase, 0.78 deep in the nematic phase, and finally 0.86 at temperatures where the smectic order is beginning to take place. The observed temperature variation of this exponent indicates an increasing role of long wavelength diffusion modes on cooling the sample. It is caused by the gradual transition of the high-temperature structure with the nonuniform planar orientation in the surface layer into a more homogeneous director field along the pore segment in the nematic phase. Independently from the exponent, the changes in the structure are indicated also by the low-frequency cutoff of the RMTD contribution. It yields the largest characteristic decay time of the orientational correlation function. The corresponding distance traveled by a molecule in this time, ℓ_{max}, is ~30 nm above T_{NI} and ~60 nm in the nematic phase, which is roughly the length of a pore

segment. At 28 °C, where the transition into the smectic-A phase has started, ℓ_{max} is smaller again. The origin of this diminishing is not clear, it might be hinting at a more complex structure related to the appearance of smectic "domains" and defects which have not been present before. The low frequency cutoff of the small ODF contribution shows that the structural changes are accompanied also by an increase in the surface anchoring strength with decreasing temperature.

Finally, the results presented in this paper show that NMR relaxometry is not able to detect director fluctuations correlated over micrometer distances and does not prove long-range order of the director orientation as suggested in Ref. [18]. Our observations, however, are in agreement with the model of independent pore segments with director parallel to the pore axis. The ultraslow fluctuations in the order parameter detected by Wu *et al.* [52] in severely constrained systems are out of the reach of our experiment.

APPENDIX: LOCAL MOLECULAR REORIENTATIONS (*R*)

The spin-lattice relaxation rate induced by local molecular reorientations is given by

$$\left(\frac{1}{T_1}\right)_R = A_{ROT}[J_1(\omega)_R + J_2(2\omega)_R]. \tag{A1}$$

Within the Woessner model, extended to the anisotropic systems, the spectral densities for the relaxation of a proton spin pair are [30–33]

$$J_k(\omega)_R = \frac{4}{3}c_k\sum_{m=-2}^{2}\frac{\overline{|d_{m0}^2(\alpha)|^2}}{a^6}\langle|D_{km}(\theta)|^2\rangle\frac{\tau_m}{1+\omega^2\tau_{|m|}^2}, \tag{A2}$$

$$c_k = \begin{cases} 6, & k=0 \\ 1, & k=1 \\ 4, & k=2. \end{cases} \tag{A3}$$

It is assumed that the director of the system is parallel to the magnetic field. In Eq. (A2), $d_{mn}^2(\alpha)$ is the second rank reduced Wigner rotation matrix and the factors $\overline{|d_{m0}^2(\alpha)|^2}/a^6$ have the form

$$\overline{\frac{|d_{m0}^2(\alpha)|^2}{a^6}} = \begin{cases} \dfrac{\overline{(3\cos^2\alpha - 1)^2}}{4a^6}, & m = 0 \\[3mm] \dfrac{\overline{3\sin^2 2\alpha}}{8a^6}, & m = 1 \\[3mm] \dfrac{\overline{3\sin^4\alpha}}{8a^6}, & m = 2, \end{cases} \qquad (A4)$$

where a is the distance between the two protons in Å and α the angle between the interproton vector and the long mo-

lecular axis. In case of 8CB we use for an estimate a =1.79 Å and $\alpha \sim 90°$ for the proton pairs in the alkyl chain (their contribution weighted by 17/25), and a=2.44 Å and $\alpha \sim 0$ for the aromatic proton pairs (their contribution weighted by 8/25). The prefactor A_{ROT} in Eq. (A1) is left as a free parameter in the fit to the bulk nematic phase in order to provide a correction to the Woessner's model of isolated spin pairs. The interactions of a spin with its next to nearest neighbors, including also those in the neighboring molecules, namely increase the effective strength of dipolar interaction. A_{ROT} obtained for the bulk nematic phase is used as a fixed parameter in other fits. Further,

$$\langle |D_{k,\pm m}|^2 \rangle = \begin{bmatrix} 7 + 10S + 18\langle P_4 \rangle - 35S^2 & 7 + 5S - 12\langle P_4 \rangle & 7 - 10S + 3\langle P_4 \rangle \\[3mm] 7 + 5S - 12\langle P_4 \rangle & 7 + \dfrac{5}{2}S + 8\langle P_4 \rangle & 7 - 5S - 2\langle P_4 \rangle \\[3mm] 7 - 10S + 3\langle P_4 \rangle & 7 - 5S - 2\langle P_4 \rangle & 7 + 10S + \dfrac{1}{2}\langle P_4 \rangle \end{bmatrix}, \qquad (A5)$$

where S and $\langle P_4 \rangle$ are the orientational order parameters expressed in terms of the second and fourth rank Legendre polynomials of the angle θ between the long molecular axis and the local nematic director:

$$S = \langle P_2 \rangle = \frac{1}{2}\langle 3\cos^2\theta - 1 \rangle,$$

$$\langle P_4 \rangle = \frac{1}{8}\langle 35\cos^4\theta - 30\cos^2\theta + 3 \rangle. \qquad (A6)$$

In the fits we use S=0.45 at 37 °C and S=0.6 at 28 °C [42]. The higher order parameter $\langle P_4 \rangle$ can be to a good approximation expressed as $5/7S^2$ [53].

The correlation times τ_m can be expressed in terms of two correlation times corresponding to molecular reorientations parallel and perpendicular to the long molecular axis, τ_L and τ_S, respectively,

$$\tau_0^{-1} = \tau_S^{-1}, \quad \tau_1^{-1} = \frac{1}{\tau_L} + \frac{1}{\tau_S},$$

$$\tau_2^{-1} = \frac{4}{\tau_L} + \frac{1}{\tau_S}. \qquad (A7)$$

The original Woessner's expression for the isotropic phase [30] is obtained by inserting S=0 and $\langle P_4 \rangle$=0 into Eq. (A5).

[1] G. S. Iannacchione, G. P. Crawford, S. Zumer, J. W. Doane, and D. Finotello, Phys. Rev. Lett. **71**, 2595 (1993).

[2] S. Kralj, G. Lahajnar, A. Zidansek, N. Vrbancic-Kopac, M. Vilfan, R. Blinc, and M. Kosec, Phys. Rev. E **48**, 340 (1993).

[3] G. S. Iannacchione, G. P. Crawford, S. Qian, J. W. Doane, D. Finotello, and S. Zumer, Phys. Rev. E **53**, 2402 (1996).

[4] T. Jin and D. Finotello, Phys. Rev. Lett. **86**, 818 (2001).

[5] M. Vilfan, B. Zalar, A. K. Fontecchio, Mojca Vilfan, M. J. Escuti, G. P. Crawford, and S. Zumer, Phys. Rev. E **66**, 021710 (2002).

[6] Ch. Cramer, Th. Cramer, F. Kremer, and R. Stannarius, J. Chem. Phys. **106**, 3730 (1996).

[7] P. Tallavaara, V. V. Telkki, and J. Jokisaari, J. Phys. Chem. B **110**, 21603 (2006).

[8] F. Grinberg, M. Vilfan, and E. Anoardo, in *NMR of Ordered Liquids*, edited by E. E. Burnell and C. A. de Lange (Kluwer Academic Publishers, Dordrecht, 2003), pp. 375–398.

[9] E. Anoardo, F. Grinberg, M. Vilfan, and R. Kimmich, Chem. Phys. **297**, 99 (2004).

[10] M. Vilfan, T. Apih, A. Gregorovic, B. Zalar, G. Lahajnar, S. Zumer, G. Hinze, R. Boehmer, and G. Althoff, Magn. Reson. Imaging **19**, 433 (2001).

[11] R. Y. Dong, Annu. Rep. NMR Spectrosc. **53**, 67 (2004).

[12] R. Kimmich, *NMR Thomography, Diffusometry, Relaxometry* (Springer, Berlin, 1997).

[13] R. Kimmich and E. Anoardo, Prog. Nucl. Magn. Reson. Spectrosc. **44**, 257 (2004).

[14] D. M. Sousa, G. D. Marques, P. J. Sebastiao, and A. C. Ribeiro, Rev. Sci. Instrum. **74**, 4521 (2003).

[15] F. Grinberg, R. Kimmich, and E. Stapf, Magn. Reson. Imaging

16, 635 (1998).

[16] M. V. Terekhov, S. V. Dvinskikh, and A. F. Privalov, Appl. Magn. Reson. **15**, 363 (1998).

[17] F. Grinberg, Magn. Reson. Imaging **25**, 485 (2007).

[18] N. Leon, J. P. Korb, I. Bonalde, and P. Levitz, Phys. Rev. Lett. **92**, 195504 (2004).

[19] P. J. Sebastiao, D. Sousa, A. C. Ribeiro, M. Vilfan, G. Lahajnar, J. Seliger, and S. Zumer, Phys. Rev. E **72**, 061702 (2005).

[20] S. Larochelle, M. Ramazanoglu, and R. J. Birgeneau, Phys. Rev. E **73**, 060702(R) (2006).

[21] R. Guegan, D. Morineau, C. Loverdo, W. Beziel, and M. Guendouz, Phys. Rev. E **73**, 011707 (2006).

[22] T. Jin, B. Zalar, A. Lebar, M. Vilfan, S. Zumer, and D. Finotello, Eur. Phys. J. E **16**, 159 (2005).

[23] D. Liang and R. L. Leheny, Phys. Rev. E **75**, 031705 (2007).

[24] A. Hourri, P. Jamee, T. K. Bose, and J. Thoen, Liq. Cryst. **29**, 459 (2002).

[25] M. R. Bengoechea, S. Basu, and F. M. Aliev, Mol. Cryst. Liq. Cryst. **421**, 187 (2004).

[26] S. Diez, M. A. Perez Jubindo, R. M. de la Fuente, D. O. Lopez, J. Salud, and L. J. Tamarit, Liq. Cryst. **33**, 1083 (2006).

[27] A. Lebar and B. Zalar (private communication).

[28] S. Kralj, A. Zidansek, G. Lahajnar, I. Musevic, S. Zumer, R. Blinc, and M. M. Pintar, Phys. Rev. E **53**, 3629 (1996).

[29] Z. Kralj, G. Cordoyiannis, A. Zidansek, G. Lahajnar, H. Amenitsch, S. Zumer, and Z. Kutnjak, J. Chem. Phys. **127**, 154905 (2007).

[30] D. E. Woessner, J. Chem. Phys. **36**, 1 (1962).

[31] V. Rutar, M. Vilfan, R. Blinc, and E. Bock, Mol. Phys. **35**, 721 (1978).

[32] P. A. Beckmann, J. W. Emsley, G. R. Luckhurst, and D. L. Turner, Mol. Phys. **50**, 699 (1983); **59**, 97 (1986).

[33] J. Dolinsek, O. Jarh, M. Vilfan, S. Zumer, R. Blinc, J. W. Doane, and G. P. Crawford, J. Chem. Phys. **95**, 2154 (1991). In Eq. (A3) of the Appendix the term $-35S^2$ is missing in the expression in the first row of the first column.

[34] P. Ukleja, J. Pirs, and J. W. Doane, Phys. Rev. A **14**, 414

(1976).

[35] H. C. Torrey, Phys. Rev. **92**, 962 (1953).

[36] S. Zumer and M. Vilfan, Phys. Rev. A **17**, 424 (1978); M. Vilfan and S. Zumer, *ibid.* **21**, 672 (1980).

[37] S. Zumer, S. Kralj, and M. Vilfan, J. Chem. Phys. **91**, 6411 (1989).

[38] M. Vilfan and M. Vuk, J. Chem. Phys. **120**, 8638 (2004).

[39] S. Stapf, R. Kimmich, and J. Niess, J. Appl. Phys. **75**, 529 (1994).

[40] R. Kimmich and H. W. Weber, Phys. Rev. B **47**, 11788 (1993).

[41] P. G. de Gennes and J. Prost, *The Physics of Liquid Crystals* (Clarendon Press, Oxford, 1993).

[42] R. Y. Dong, *Nuclear Magnetic Resonance of Liquid Crystals*, 2nd ed. (Springer, Berlin, 1997), and references therein.

[43] A. Carvalho, P. J. Sebastiao, A. C. Ribeiro, H. T. Nguyen, and M. Vilfan, J. Chem. Phys. **115**, 10484 (2001).

[44] P. Ziherl, M. Vilfan, and S. Zumer, Phys. Rev. E **52**, 690 (1995).

[45] M. Abramowitz and I. A. Stegun, *Handbook of Mathematical Functions* (Dover, New York, 1972).

[46] There is a difference in the numerical prefactor, which is $2^{-(d+2)}[\sin(d\pi/4)]^{-1}$ in the present paper and $2^{-(d+3/2)}$ in Ref. [18]. Using the latter prefactor does not lead to the correct limit in the two-dimensional case. However, in the whole dimensionality range from 1 to 3, the discrepancy in the relaxation rates caused by the prefactors does not exceed ~25%.

[47] F. Bonetto, E. Anoardo, and R. Kimmich, J. Chem. Phys. **118**, 9037 (2003).

[48] S. V. Dvinskikh, I. Furo, H. Zimmermann, and A. Maliniak, Phys. Rev. E **65**, 061701 (2002).

[49] G. Schwalb and F. W. Deeg, Phys. Rev. Lett. **74**, 1383 (1995).

[50] H. Gotzig, S. Grunenberg-Hassanien, and F. Noack, Z. Naturforsch., A: Phys. Sci. **49a**, 1179 (1994).

[51] H. Hakemi, Liq. Cryst. **5**, 334 (1989).

[52] X-L. Wu, W. I. Goldburg, M. X. Liu, and J. Z. Xue, Phys. Rev. Lett. **69**, 470 (1992).

[53] U. Fabbri and C. Zannoni, Mol. Phys. **58**, 763 (1986).